

The HLS approach to $(g - 2)_\mu$: A Solution to the “ τ versus e^+e^- ” Puzzle

Maurice Benayoun^{1,a,b}

¹LPNHE des Universités Paris VI et Paris VII, IN2P3/CNRS, 4 Place Jussieu, 75252 Paris, France

Abstract. The Hidden Local Symmetry (HLS) Model provides a framework able to encompass several physical processes and gives a unified description of these in an energy range extending up to the ϕ mass. Supplied with appropriate symmetry breaking schemes, the HLS Model gives a broken Effective Lagrangian (BHLS). The BHLS Lagrangian gives rise to a fit procedure in which a simultaneous description of the e^+e^- annihilations to $\pi^+\pi^-$, $\pi^0\gamma$, $\eta\gamma$, $\pi^+\pi^-\pi^0$, K^+K^- , K_LK_S and of the dipion spectrum in the decay $\tau^\pm \rightarrow \pi^\pm\pi^0\nu$ can be performed. Supplemented with a few pieces of information on the $\rho^0 - \omega - \phi$ system, the τ dipion spectrum is shown to predict accurately the pion form factor in e^+e^- annihilations. Physics results derived from global fits involving or excluding the τ dipion spectra are found consistent with each others. Therefore, no obvious mismatch between the τ and e^+e^- physics properties arises and the $\tau - e^+e^-$ puzzle vanishes within the broken HLS Model.

1 Introduction

The pion form factor in the $e^+e^- \rightarrow \pi^+\pi^-$ annihilation ($F_\pi^{ee}(s)$) and in the $\tau^\pm \rightarrow \pi^\pm\pi^0\nu$ decay ($F_\pi^\tau(s)$) are expected to differ only by isospin symmetry breaking (IB) terms. Understanding the relationship between $F_\pi^{ee}(s)$ and $F_\pi^\tau(s)$ is important as it can allow for 2 different evaluations of the dipion contribution to $a_\mu(\pi\pi)$, the muon Hadronic Vacuum Polarization (HVP) which could be merged together if consistent with each other. However, this relationship supposes a good understanding of isospin symmetry breaking and an appropriate modelling.

For a long time [1, 2], the comparison between $|F_\pi^{ee}(s)|^2$ and $|F_\pi^\tau(s)|^2$ was not satisfactory and the mismatch [3] was severe enough that one started to speak of a “ e^+e^- vs τ ” puzzle. This has continued up to very recently [4]. However, some works [5, 6] indicated that this puzzle could well be a modelling issue of the isospin symmetry breaking phenomenon. On the other hand, it was also shown [7] that, numerically, the $e^+e^- - \tau$ discrepancy sensitively depends on the $e^+e^- \rightarrow \pi^+\pi^-$ sample considered. Therefore the so-called $e^+e^- - \tau$ puzzle may carry several components.

The Hidden Local Symmetry (HLS) Model provides a framework and a procedure able to address this puzzle in the various aspects just sketched. The HLS model encompasses several physical processes and gives a unified description of these in an energy range extending up to the ϕ mass. However, in order to account precisely for experimental data, it should be supplied with several symmetry breaking schemes. Among these, an energy dependent mixing mechanism of the neutral vector meson system ($\rho^0 - \omega - \phi$) is generated via loop effects and allows

to define an effective broken HLS (BHLS) model. Within this framework, the e^+e^- annihilations to $\pi^+\pi^-$, $\pi^0\gamma$, $\eta\gamma$, $\pi^+\pi^-\pi^0$, K^+K^- , K_LK_S and the dipion spectrum in the decay $\tau^\pm \rightarrow \pi^\pm\pi^0\nu$ are *simultaneously* accounted for with the same set of parameters derived from global fits in procedures involving all the existing data samples covering the channels listed above. One can also define a variant – named $\tau + \text{PDG}$ – where the $e^+e^- \rightarrow \pi^+\pi^-$ data are replaced by tabulated ρ^0 , ω and ϕ particle properties[18]; with such a tool, one can compare the τ predictions for the $e^+e^- \rightarrow \pi^+\pi^-$ annihilation and the data. If the $e^+e^- - \tau$ puzzle is a relevant concept, this comparison should enhance the issue.

After a brief review of the BHLS Model and its breaking in Sections 2, 3 and 4, the various aspects of the global fit method are outlined in Section 5. Section 6 studies the $\tau + \text{PDG}$ predictions and their comparison with the existing $e^+e^- \rightarrow \pi^+\pi^-$ data samples. In Section 7, one reports on global fits mixing $e^+e^- \rightarrow \pi^+\pi^-$ and τ dipion data. In Section 8, the effects of τ data on the muon HVP are discussed. Section 9 is devoted to the conclusions.

2 Basics of the Hidden Local Symmetry Model

The Hidden Local Symmetry Model (HLS) Model is a framework which encompasses simultaneously several different physics processes covered by a large number of already available data samples. A comprehensive review of the HLS Model is given in [8] and a brief account can be found in [9]; however, in order to really deal with experimental data at their present level of accuracy, breaking procedures need to be implemented. As these are tightly connected with the HLS Model structure, it is worth giving a brief outline of its main features.

^ae-mail: benayoun@in2p3.fr

^be-mail: maurice.benayoun@gmail.com

Beside its non-anomalous sector, which allows to address some e^+e^- annihilation channels and some τ decays, the HLS Model also contains an anomalous (FKTUY) sector [8, 10] which provides couplings of the form VVP , $VPPP$, γPPP , $VP\gamma$ or $P\gamma\gamma$ among the light flavor mesons¹. Intrinsically, the HLS validity range does not extend much beyond the ϕ mass.

The $e^+e^- \rightarrow \pi^+\pi^-/K\bar{K}$ annihilations or the $\tau^\pm \rightarrow \pi^\pm\pi^0\nu$ decay clearly proceed from only the non-anomalous sector of the HLS model. However, the radiative meson decays ($VP\gamma$ or $P\gamma\gamma$ couplings) as well as the annihilation channels like $e^+e^- \rightarrow \pi^0\gamma$, $e^+e^- \rightarrow \eta\gamma$ or $e^+e^- \rightarrow \pi^0\pi^+\pi^-$ involve couplings only available from the anomalous (FKTUY) sector of the HLS model.

The construction of the HLS Lagrangian starts by defining the (right and left) ξ fields :

$$\xi_{R,L} = \exp[\pm iP/f_\pi] \quad (1)$$

where f_π is the pion decay constant and $P = P_8 + P_0$ is the U(3) matrix of the pseudoscalar fields which includes the octet and singlet field components [9].

The HLS non-anomalous Lagrangian is defined by² :

$$\begin{cases} \mathcal{L}_{HLS} = \mathcal{L}_A + a\mathcal{L}_V \\ \mathcal{L}_A = -\frac{f_\pi^2}{4} \text{Tr}[(D_\mu\xi_L\xi_L^\dagger - D_\mu\xi_R\xi_R^\dagger)^2] \equiv -\frac{f_\pi^2}{4} \text{Tr}[L - R]^2 \\ \mathcal{L}_V = -\frac{f_\pi^2}{4} \text{Tr}[(D_\mu\xi_L\xi_L^\dagger + D_\mu\xi_R\xi_R^\dagger)^2] \equiv -\frac{f_\pi^2}{4} \text{Tr}[L + R]^2 \end{cases} \quad (2)$$

These expressions involve the covariant derivatives of the $\xi_{R,L}$ fields :

$$\begin{cases} D_\mu\xi_L = \partial_\mu\xi_L - igV_\mu\xi_L + i\xi_L\mathcal{L}_\mu \\ D_\mu\xi_R = \partial_\mu\xi_R - igV_\mu\xi_R + i\xi_R\mathcal{R}_\mu \end{cases} \quad (3)$$

which introduce the usual bare vector field matrix³ V ; the other gauge bosons of the Standard Model (A , W^\pm and Z) are hidden inside \mathcal{L}_μ and \mathcal{R}_μ ; neglecting the influence of the Z boson field absent from the physics we address, these are written as :

$$\begin{cases} \mathcal{L}_\mu = eQA_\mu + \frac{g_2}{\sqrt{2}}(W_\mu^+T_+ + W_\mu^-T_-) \\ \mathcal{R}_\mu = eQA_\mu \end{cases} \quad (4)$$

The quark charge matrix Q is standard and the matrix $T_+ = [T_-]^\dagger$ is constructed out of matrix elements of the Cabibbo-Kobayashi-Maskawa matrix [8]. Concerning the physics parameters, the above expressions exhibit the electric charge e , the universal vector coupling g and the weak coupling g_2 (related to the Fermi constant by $g_2 = 2m_W \sqrt{G_F \sqrt{2}}$). Finally, a is a specific HLS parameter not fixed by the model and expected of the order of 2.

¹In the following, V and P denote generically any of the resp. vector and pseudoscalar light flavor mesons and, also, the corresponding field matrices without ambiguities.

²Within the present one page reminder, we do not discuss the anomalous sectors and refer the interested reader to [8] or [9].

³Which involves the so-called ideal combinations ρ_I^0 , ω_I and ϕ_I for the neutral fields.

3 Usual symmetry-breaking schemes of the HLS Model

The HLS model obviously provides an elegant unified framework which covers an important set of annihilation and decay processes. However, as such, it cannot produce a satisfactory account of the real experimental data falling into its scope. A simple illustration is given by the pion and kaon decay constants found of equal magnitudes within the unbroken HLS Lagrangian.

This clearly indicates that symmetry breaking mechanisms should be supplied. The authors of the HLS Model were aware of this difficulty and soon proposed a simple (BKY) mechanism to break the flavor SU(3) symmetry [11] of the model; this has been later extended to include isospin breaking [12]; for practical purpose, we use the BKY mechanism as reformulated in [13]. This turns out to modify Eqs. (2) by introducing breaking matrices in the following way :

$$\begin{cases} \mathcal{L}_A = -\frac{f_\pi^2}{4} \text{Tr}[(L - R)X_A]^2 \\ \mathcal{L}_V = -\frac{f_\pi^2}{4} \text{Tr}[(L + R)X_V]^2 \end{cases} \quad (5)$$

where X_A and X_V are real diagonal matrices :

$$\begin{cases} X_A = \text{Diag}(q_A, y_A, z_A) \\ X_V = \text{Diag}(q_V, y_V, z_V) \end{cases} \quad (6)$$

which should be derived from data.

The departures of $q_{A/V}$ and $y_{A/V}$ from 1 measure the isospin symmetry breaking, while $z_{A/V}$ carry the flavor SU(3) symmetry breaking. Together with determinant terms [14] which permit to break nonet symmetry in the pseudoscalar sector, this provides a reliable description of the light meson radiative decays and of the $e^+e^- \rightarrow P\gamma$ annihilations.

4 Vector field mixing, a new symmetry breaking mechanism

The coupling of the neutral vector mesons carrying no open strangeness to a pseudoscalar meson pair is given by the following piece of the \mathcal{L}_V HLS Lagrangian⁴ [5] :

$$\begin{aligned} & \frac{iag}{2} \rho_I^0 \pi^- \overleftrightarrow{\partial} \pi^+ + \frac{iag}{4z_A} (\rho_I^0 + \omega_I - \sqrt{2}z_V\phi_I) K^- \overleftrightarrow{\partial} K^+ \\ & + \frac{iag}{4z_A} (\rho_I^0 - \omega_I + \sqrt{2}z_V\phi_I) K^0 \overleftrightarrow{\partial} \bar{K}^0 \end{aligned} \quad (7)$$

The last two terms obviously give rise to pseudoscalar kaon loops which modify the vector mass matrix by s -dependent terms. Moreover, the kaon loops generate transitions among the ideal ρ_I , ω_I and ϕ_I of the original Lagrangian and, thus, give *non-diagonal* entries inside the vector meson squared mass matrix [5, 9]. Stated otherwise, at one-loop order, the ideal ρ_I , ω_I and ϕ_I fields are no longer mass eigenstates as expected for the physical

⁴The isospin breaking effects generated by the X_A and X_V matrices have been removed for clarity; they can be found in [9].

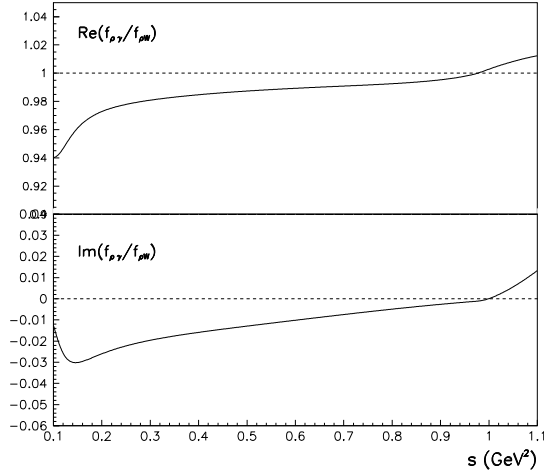


Figure 1. The ratio $f_{\rho^0\gamma}(s)/f_{\rho^\pm W}$ derived from a BHLS global fit over the region from the two-pion threshold to slightly above the ϕ mass.

vector-meson fields. The one-loop order mass squared matrix can be written as :

$$\begin{cases} M^2(s) = M_0^2(s) + \delta M^2(s) & \text{with :} \\ M_0^2(s) = \text{Diag}(m^2 + \Pi_{\pi\pi}(s), m^2, z_V m^2). \end{cases} \quad (8)$$

where $\delta M^2(s)$ is a non-diagonal perturbation matrix depending on the kaon loops to the (otherwise) diagonal matrix $M_0^2(s)$. The entries of $M_0^2(s)$ depend on m^2 – the squared ρ (or ω) meson mass, as it occurs in the original HLS Lagrangian – and on $\Pi_{\pi\pi}(s)$, the dipion loop to which only ρ_I couples.

As $\delta M^2(s)$ is small compared to $M_0^2(s)$ within the range of validity of the HLS model (*i.e.* up to the ϕ mass region), the eigenvalue problem Eq. (8) can be solved perturbatively. The relation between the ideal fields (V_I) and the physical fields (V_R) can be written :

$$\begin{pmatrix} \rho_I \\ \omega_I \\ \phi_I \end{pmatrix} = \begin{pmatrix} 1 & -\alpha & \beta \\ \alpha & 1 & \gamma \\ -\beta & -\gamma & 1 \end{pmatrix} \begin{pmatrix} \rho_R^0 \\ \omega_R \\ \phi_R \end{pmatrix} \quad (9)$$

where α , β and γ are functions of s , the energy flowing through the vector meson line. These functions essentially⁵ depend on the sum and the difference of the charged and neutral kaon loops and are small compared to 1 [5, 9]. Therefore, the vector field mixing mechanism introduces breaking terms which are s -dependent, s being the running vector meson mass.

This change of fields is what mostly generates an isospin 1 component inside the physical ω and ϕ mesons

⁵Actually, $K^*\bar{K}$ and $K^*\bar{K}^*$ loops are provided by resp. the VVP anomalous Lagrangian and by the Yang-Mills term; however, up the ϕ mass region they are real and effectively absorbed inside the subtraction polynomials of the kaon loop combinations.

and, then, their couplings to a pion pair as, using Eq. (9), one gets at first order in breaking parameters⁶ :

$$\frac{ia g}{2} \rho_I \cdot \pi^- \overleftrightarrow{\partial} \pi^+ \Rightarrow \frac{ia g(1 + \Sigma_V)}{2} \left[\rho_R^0 + [(1 - h_V)\Delta_V - \alpha(s)\omega + \beta(s)\phi] \right] \cdot \pi^- \overleftrightarrow{\partial} \pi^+ \quad (10)$$

At this order, the ρ_R^0 coupling to a pion pair is unchanged and remains identical to those of the ρ^\pm meson. On the other hand, the change of fields Eq. (9) modifies the Lagrangian coupling of the neutral ρ meson to the photon, while leaving unchanged the charged ρ coupling to the W boson. Therefore, the vector field mixing makes the ratio of these two couplings s -dependent :

$$\frac{f_{\rho^0\gamma}(s)}{f_{\rho^\pm W}} = \left[1 + \frac{h_V\Delta_V}{3} + \frac{\alpha(s)}{3} + \frac{\sqrt{2}z_V}{3}\beta(s) \right]. \quad (11)$$

In order to substantiate this specific breaking of the HLS model, let us quote a result derived from a global fit involving all the channels listed in the Introduction; the ratio $f_{\rho^0\gamma}(s)/f_{\rho^\pm W}$ shown in Figure 1 exhibits significant variations over the HLS energy range of interest. It is the main mechanism which allows to reconcile the τ dipion spectrum and the $e^+e^- \rightarrow \pi^+\pi^-$ annihilation cross section. These couplings are supplemented by loop corrections [5, 9] which also play an important role in defining the effective γV mixings⁷.

On the other hand, the τ decay process also undergoes several specific breaking effects : The short range [15] and long range [16] corrections are included when fitting the τ dipion spectrum, as for the specific $\pi^\pm\pi^0$ phase space factor. These τ breaking effects are accounted for within fits as usually done; they are clearly independent of the HLS breaking mechanisms and only come supplementing them.

5 The various aspects of the global fit method

Gradually equipped since [5] with the various breaking procedures briefly outlined above, the HLS Model has evolved toward a broken version (BHLS) [9] able now to cope simultaneously with several physics processes, namely the e^+e^- annihilations to $\pi^+\pi^-$, $\pi^0\gamma$, $\eta\gamma$, $\pi^+\pi^-\pi^0$, K^+K^- , $K_L K_S$, the dipion spectrum in the decay $\tau^\pm \rightarrow \pi^\pm\pi^0\nu$ and, additionally, some more radiative decays of light flavor mesons. It involves 25 parameters to be extracted from data and they come intricately simultaneously within the various amplitudes.

Therefore, BHLS is a global model permitting a global account of all the processes just listed. As the *same* model parameters are involved in the *different* physics processes, this implies the existence of *physics* correlations among the various spectra or partial widths entering the BHLS realm.

⁶The Δ_V comes from an additional (minor) breaking process [9]; Δ_V and Σ_V are combinations of the breaking parameters q_V and y_V generated by the BKY mechanism.

⁷See also [6].

One obviously expects herefrom an improvement of the knowledge of the physics model parameters involved in each given channel \mathcal{I} , as the experimental data covering the other (different) channels contribute to improve the uncertainties of each of the model parameters and, hence, the statistical quality of the account of \mathcal{I} . Of course, the fit quality is expected to reflect that the physics constraints exhibited by the (BHLS) model are well accepted by the data.

The number of independent data samples covering the various quoted channels is of the order of 50; they are listed and discussed in [9]. In this Reference, a simultaneous fit of all available e^+e^- annihilation scan data and of the published τ dipion spectra is performed. A very good fit quality is reached and no noticeable issue is observed. As the model is global, it also represents a new tool to examine precisely several issues [17] :

1. The discrepancy between the dipion spectrum in the τ decay and in the e^+e^- annihilation;
2. The relative compatibility of the various available $e^+e^- \rightarrow \pi^+\pi^-$ cross section measurements up to the ϕ mass;
3. The compatibility of the τ and e^+e^- based estimates of the hadronic vacuum polarization (HVP) contribution to the muon $g - 2$.

The following sections outline the BHLS analysis of these issues.

6 The BHLS prediction of the pion form factor in e^+e^- annihilations

Since 2002 several measurements of the pion form factor in e^+e^- annihilations have been published. Beside the data samples collected in scan mode by CMD-2 [19] and SND [20], the KLOE Collaboration has produced three spectra collected in the ISR mode under different conditions, namely KLOE08 [21], KLOE10 [22] and recently the KLOE12 data sample [23] – strongly correlated with KLOE08. BaBar has also produced a $\pi^+\pi^-$ spectrum [24] extending up to 1.8 GeV. Finally, very recently, the BES-III Collaboration has published a new spectrum [25] limited to the energy interval 0.6 – 0.9 GeV. Except for the BES-III data sample presented in [27], these data samples have been examined in either of [17] or [26] – specifically for the KLOE12 sample. The present study outlines the treatment of the BES-III sample within the BHLS fitter.

A priori, BHLS can predict the pion form factor in the $e^+e^- \rightarrow \pi^+\pi^-$ annihilation relying on the measured τ dipion spectra [28–30], provided it is also fed with the appropriate isospin breaking (IB) information. However, despite the intricacy phenomenon noted above, some of the specific IB effects occurring in the $e^+e^- \rightarrow \pi^+\pi^-$ annihilation are marginally constrained by the other annihilation channels included within the BHLS realm. So, specific data directly reflecting these IB effects should be provided

to the BHLS fitter. Such pieces of information are obviously related with the $\omega/\phi \rightarrow \pi^+\pi^-$ couplings. Reference [17] proposed to use the corresponding tabulated [18] partial widths and the (Orsay) phases between the ω/ϕ amplitudes and the underlying coherent $\pi^+\pi^-$ background; this phase information can be replaced by the relevant tabulated products $\Gamma(V \rightarrow e^+e^-) \times \Gamma(V \rightarrow \pi^+\pi^-)$. Additionally, as the $\rho^0 \rightarrow e^+e^-$ coupling is marginally constrained by the non- $\pi^+\pi^-$ annihilation data, one should include the tabulated $\rho^0 \rightarrow e^+e^-$ decay width. This method is named τ +PDG for obvious reasons⁸.

For reasons which will become clear soon, it deserves noting that none of the 5 pieces of information supplementing the τ spectra in the τ +PDG approach is influenced by any of the KLOE, BaBar or BES-III $\pi^+\pi^-$ spectra. Actually, they are almost 100% determined by the data collected by the CMD-2 and SND Collaborations.

The red curve in Figure 2 displays the τ +PDG distribution and, superimposed, all the available $e^+e^- \rightarrow \pi^+\pi^-$ data samples. When MINUIT has converged, one can compute the χ^2 distance of each of the available $\pi^+\pi^-$ spectra to the τ +PDG best fit function; the average χ^2 per data point is then calculated for each data sample and all are reported inside the plots as comments⁹.

Obviously, the left-hand side panel indicates that, overall, the agreement between the τ +PDG prediction and the data is satisfactory, and the inset indicates that this agreement extends to the close spacelike region¹⁰. Therefore, the accepted (PDG) values for the IB pieces of information listed above allow to recover the gross features of the pion form factor with a noticeable precision; this already indicates that the IB mechanism as plugged within BHLS is appropriate.

The right-hand side panel, however, indicates that we are faced with a contrasting picture, depending on the data samples examined. As a good tag of the agreement between the BHLS τ +PDG and the (secure) NSK data¹¹, the relevant subpanel in the right-hand side of Figure 2 displays the average χ^2 distance per data point of the NSK samples; one gets $\bar{\chi}_{NSK}^2 = 1.2$, close to the best fit value in a fit where the PDG information is replaced by the CMD-2 and SND $e^+e^- \rightarrow \pi^+\pi^-$ data samples [9]. This also gives a hint about the range of acceptable values for the $\bar{\chi}^2$ associated with any given sample.

Therefore, the BHLS fit in the τ +PDG mode provides IB parameter values which allow the underlying (BHLS) IB framework to exhibit a full consistency of all non $\pi^+\pi^-$ data with the $\pi^+\pi^-$ NSK (*i.e.* CMD-2 & SND) data. The

⁸It should nevertheless be kept in mind that the annihilation cross-sections to $\pi^0\gamma, \eta\gamma, \pi^+\pi^-\pi^0, K^+K^-$ and K_LK_S are always fully involved within the global fit. They mainly serve to fit the γV transition amplitudes also involved in the $e^+e^- \rightarrow \pi^+\pi^-$ annihilation process.

⁹Quite generally, the CMD-2 and SND data samples are grouped together and denoted NSK; to avoid energy calibration issues around the ω mass, the χ^2 value shown for BaBar is calculated by amputating the spectrum from its part falling between 0.76 and 0.80 GeV.

¹⁰It is nevertheless premature to include this region inside the BHLS fit [27].

¹¹The NSK data are implicitly (or explicitly) considered as a reference, as they can accommodate *separately* almost all the other data samples with, however, various qualities.

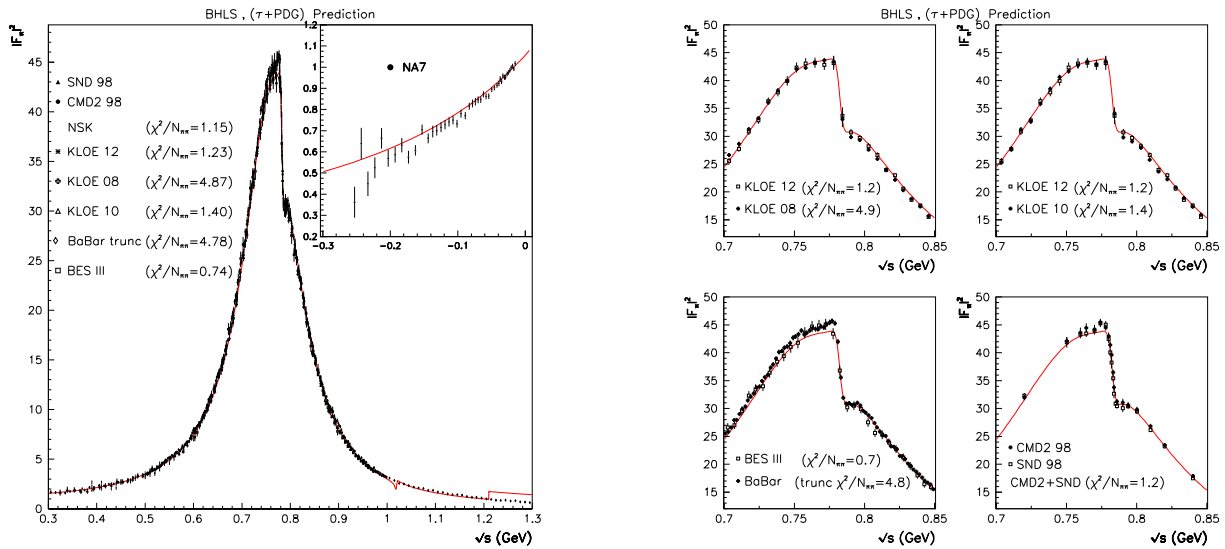


Figure 2. Predictions for the pion form factor in the $e^+e^- \rightarrow \pi^+\pi^-$ annihilation derived using the τ + PDG method. None of the $\pi^+\pi^-$ spectra is used in the fitting procedure. The leftmost panel displays the overall picture with data superimposed, the inset showing the form factor continuation into the spacelike ($s < 0$) region. The rightmost panel displays, enlarged, the behavior of the various data samples in the $\rho - \omega$ interference region.

picture is clearly alike for the KLOE10 ($\bar{\chi}^2_{KLOE10} = 1.4$), KLOE12 ($\bar{\chi}^2_{KLOE12} = 1.2$) and BES-III ($\bar{\chi}^2_{BES} = 0.7$) data samples. In contrast, one observes that the KLOE08 ($\bar{\chi}^2_{KLOE08} = 4.9$) or BaBar ($\bar{\chi}^2_{BaBar\ trunc} = 4.8$) samples are farther than could be expected.

The upper left-hand plot in the right panel of Figure 2 is also quite informative; indeed it shows that the twin samples KLOE08 and KLOE12 [21, 23] carry central values very close to each other and that both follow almost exactly the τ +PDG predicted curve. Nevertheless, KLOE12 exhibits a $\bar{\chi}^2$ value in close agreement with the τ +PDG expectations while KLOE08 does not. This should be due to the estimates and structure of the reported correlated systematic uncertainties, seemingly better understood for the KLOE12 sample.

Finally, there is a clear contradiction between the KLOE and BaBar samples, as already reported by other authors (see for instance [7]) but, also, BaBar does not fit well with the BHLS τ +PDG predictions.

Therefore, as in the comparison between the τ +PDG predictions and the various $\pi^+\pi^-$ data samples, five out of the seven available independent $\pi^+\pi^-$ samples do not exhibit any kind of mismatch, one is obviously tempted to conclude that there is no evidence for a $\tau - e^+e^-$ puzzle. The BHLS approach would rather indicate that the reported puzzle comes from a non-adequate IB modelling.

7 The BHLS global fits

So, the comparison between the τ predictions – also based on commonly accepted PDG information – and the various $\pi^+\pi^-$ data samples indicates various behaviors. More precisely, the τ + PDG method gives a well-founded

indication that the CMD-2, SND, KLOE10, KLOE12 and BES-III $e^+e^- \rightarrow \pi^+\pi^-$ data samples should be quite consistent with the τ dipion spectra; in contrast, one may expect that KLOE08 and BaBar should exhibit some difficulty to accommodate the τ spectra within the BHLS framework. A step further is to perform global fits within the BHLS framework including the τ spectra and the various $e^+e^- \rightarrow \pi^+\pi^-$ data samples, each in isolation or in combinations. The results obtained should allow for more conclusive statements.

The first data line in Table 1 reports some fit information derived using the various $\pi^+\pi^-$ samples in isolation, namely their various $\bar{\chi}^2$ and their global fit probabilities¹²; in these fits, the PDG information previously referred to should be removed. One observes a significant gap between KLOE08 and BaBar, on the one hand and the five other data samples, on the other hand¹³.

In the same Table, one also displays the fit results associated with different combinations of the existing data samples. This Table shows that the largest set where each data sample has an average $\bar{\chi}^2$ per point close to its value in its single mode fit is Combination 1; this combination is our reference for the following. For this combination, the $\bar{\chi}^2$ of the whole set of $\pi^+\pi^-$ data sample is 0.98 with an associated large probability as indicated in the first column.

The pion form factor (FF) in e^+e^- annihilations and in the τ decay derived from fitting with Combination 1 are

¹²As illustrated by Table 3 in [9] and reminded in [17, 27], the global fit probabilities are enhanced towards 1 because several groups of data samples – especially those collected in the $\pi^0\gamma$ and $\eta\gamma$ channels – benefit from very favorable partial $\bar{\chi}^2$. Under these conditions, small global probabilities indicate suspicious behaviors.

¹³The quantity denoted $\lambda^2_{\pi^+\pi^-}$ is, of course, the contribution to the total $\bar{\chi}^2$ of the $\pi^+\pi^-$ data.

Table 1. Fit mixing the indicated $e^+e^- \rightarrow \pi^+\pi^-$ samples and the τ spectra in single mode or combined. The values are the ratios $\chi^2/N_{\pi^+\pi^-}$ returned by the fits and the global fit probability are given for each data sample or for the selected sample combinations.

Fit Cond.	KLOE08	KLOE10	KLOE12	NSK	BES-III	BaBaR (trunc)	BaBaR (full)
Single $\chi^2/N_{\pi^+\pi^-}$	1.64	0.96	1.02	0.96	0.56	1.15	1.25
(prob)	(59%)	(97%)	(97%)	(97%)	(99%)	(74%)	(40%)
Comb. 1 (0.98 [99%])	–	1.00	1.05	1.11	0.61	–	–
Comb. 2 (1.06 [97%])	–	1.02	1.05	1.10	–	–	–
Comb. 3 (1.21 [22%])	–	1.01	1.54	1.18	0.56	1.36	–

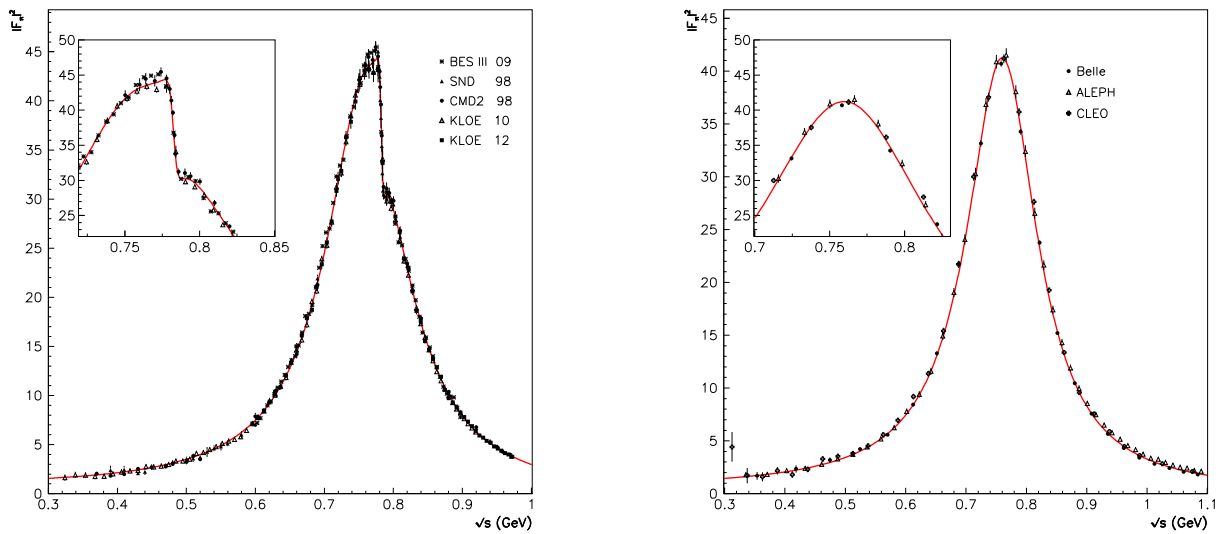


Figure 3. The pion form factor in the $e^+e^- \rightarrow \pi^+\pi^-$ annihilation (left-hand panel) and in the τ decay (right-hand panel) derived from a BHLS fit involving the CMD-2, SND, KLOE10, KLOE12 and BES-III data samples, on the one hand, and the ALEPH, CLEO and Belle dipion spectra, on the other hand.

displayed in Figure 3; they are clearly satisfactory. The older $\pi^+\pi^-$ data reported in [31] are also included in the fit and, on the whole, one yields $\chi^2_{\pi^+\pi^-}/N_{\pi^+\pi^-} = 361.5/404$ and $\chi^2_{\pi^+\pi^0}/N_{\pi^+\pi^0} = 86.8/85$. Therefore the picture looks satisfactory and this should be reflected by the residual plots.

Figure 4 displays the e^+e^- pion FF residuals appropriately corrected for the reported scale uncertainty effects as discussed in the Appendix of [17] and in [27]; it looks reasonably flat.

The pion FF in the τ decay is flat for the CLEO and Belle spectra¹⁴; the ALEPH data sample tends to exhibit a small growth starting at $\simeq 850$ MeV. However, Figure 3 in [32] indicates that this distribution, thanks to a bug fix, should be scaled down just in this energy region and, then, it behaves like the others.

Therefore, the global fits mixing the τ spectra and the $e^+e^- \rightarrow \pi^+\pi^-$ data samples confirm the conclusions reached in the previous Section with the τ + PDG method.

¹⁴Actually, the 3 residual distributions shown in the lower panel of Figure 4 look quite similar to the Belle plots displayed in Figure 12 of [30].

Stated otherwise, global fits do not indicate any mismatch between the e^+e^- and τ spectra within BHLS.

8 Including & excluding the τ spectra : Hadronic HVP issues

Let us first examine the contributions to the muon HVP provided by the pion loop in the energy region [0.630,0.958] GeV; Figure 5 displays our results. The point at top of this Figure displays the τ +PDG prediction for $a_\mu(\pi\pi, [0.63, 0.958])$. The data points in red display the corresponding information directly reconstructed from the samples provided by the indicated experiments; some combinations of these are also shown. So, one observes a quite good correspondance between the "experimental" values and the prediction derived by the τ +PDG method; of course, the experimental values are not influenced at all by BHLS or the τ data.

In the same Figure, one also displays the results derived when merging the $e^+e^- \rightarrow \pi^+\pi^-$ data samples and the τ dipion spectra in the minimization procedure. The empty black symbols show the fit results derived by using the iterative method defined in [27]. The points in green

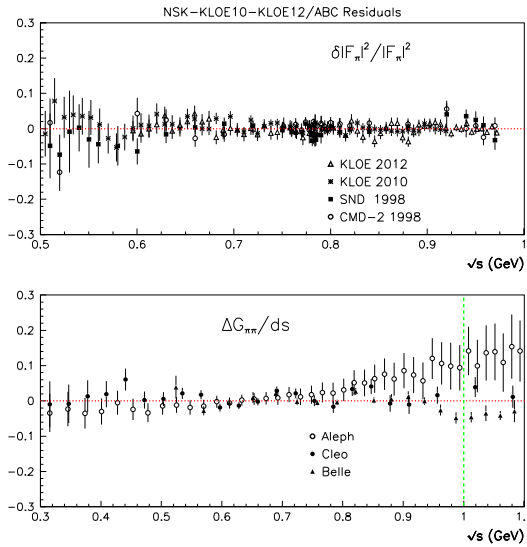


Figure 4. Residuals for the pion form factor in the $e^+e^- \rightarrow \pi^+\pi^-$ annihilation (upper panel) and in the τ decay (lower panel). The residuals in the upper panel are corrected for the global scale uncertainty effects (see [17, 27]).

are the corresponding results derived from the same fits but performed without iterating. The motivation for an iterative method are emphasized in [27] and aims at cancelling out possible biases affecting the channels dominated by samples subject to dominant global scale uncertainties

Figure 5 shows that the τ +PDG prediction as well as the fits merging τ and e^+e^- data are consistent with each others and also with the experimental data, except for BaBar which has difficulties to accommodate the BHLS framework as shown in Table 1. Because of the energy boundaries of its spectrum, a BES-III experimental value for $a_\mu(\pi\pi, [0.63, 0.958])$ cannot be produced.

Let us go a step further and examine the contributions to the muon HVP accessible through the BHLS Lagrangian and fitting procedure which is, as already stated, limited upward slightly above the ϕ mass; we chose 1.05 GeV. The results are displayed in Table 2. The numbers have been derived using the iterated fit method already referred to [27].

Let us focus on the $\pi^+\pi^-$ contribution which is actually the main aim of the present study. One thus observes that including the τ spectra shifts the central value by about 1.5×10^{-10} and improves the uncertainty by about 0.3×10^{-10} in both cases. The 1.5×10^{-10} difference between excluding and including the τ spectra looks rather small ($\approx 1 \sigma$ or less), similar to those obtained in [6], but much smaller than those in [4]. Therefore, within BHLS, the contribution of the $\pi^+\pi^-$ channel to the HVP does not exhibit any singular behavior : Using or not the τ spectra does not change this picture but improves the results as expected from having a larger statistics (e.g. the $\pi^+\pi^-$ and the τ data).

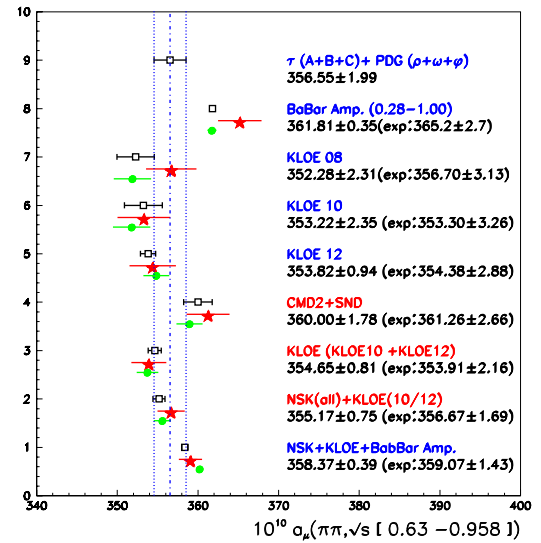


Figure 5. Values for $a_\mu(\pi\pi, [0.63, 0.958])$ in units of 10^{-10} derived from global fits using the indicated $e^+e^- \rightarrow \pi^+\pi^-$ data samples or combinations; the τ dipion spectra are always used. The full green circles are the results obtained from the $A = m$ fit (no iteration) and the black empty squares are the results obtained from the $A = M_0$ fit (first iteration) s explained in [27]. The values derived by directly integrating the experimental spectra are indicated by red stars. See Section 8 for comments.

9 Conclusion

The analysis developed above leads to conclude that, actually, one does not observe any mismatch between the e^+e^- and the τ data. To be as precise as possible, Table 1 indicates that the τ spectra collected by ALEPH, CLEO and Belle are in perfect agreement with the CMD-2, SND, KLOE10, KLOE12 and BES-III data samples¹⁵ each taken in isolation or considered together within a sample combination. This leads us to conclude that the so-called $\tau - e^+e^-$ puzzle is only due to the way the implementation of isospin symmetry breaking is performed within some models. In contrast, the BHLS approach and its way to account for IB effects seem to reflect correctly the expected relationship and the expected closeness of the e^+e^- annihilation and τ decay processes. Indeed, BHLS provides successful τ predictions of the e^+e^- pion form factor and a good simultaneous fit of both kinds of data.

However, we are left with a significant tension between the KLOE08 and BaBar (up to 1 GeV) samples on the one hand and the τ spectra on the other hand, as well reflected by the τ +PDG information collected in Figure 2 and by the BHLS global fit results displayed in Table 1. This is indeed an issue but, seemingly, external to the so-called $\tau - e^+e^-$ puzzle which motivates this work.

¹⁵As, for example, five out of the seven high statistics existing data samples.

Table 2. The various contributions to the muon HVP a_μ in units of 10^{-10} using the BHLS fit excluding the τ data (first data column), including the τ spectra (second data column), compared with the direct integration of the experimental spectra (last data column). The last line displays the total contribution accessible through the BHLS Model. The e^+e^- data samples involved are those from CMD-2, SND, KLOE10, KLOE12 and BES-III.

Channel	Excl. τ	Incl. τ	Direct Estim.
$\pi^+\pi^-$	493.02 ± 1.16	494.59 ± 0.89	492.98 ± 3.38
$\pi^0\gamma$	4.50 ± 0.05	4.54 ± 0.04	3.67 ± 0.11
$\eta\gamma$	0.64 ± 0.01	0.64 ± 0.01	0.56 ± 0.02
$\pi^+\pi^-\pi^0$	40.84 ± 0.62	40.84 ± 0.57	43.54 ± 1.29
$K_L K_S$	11.53 ± 0.09	11.53 ± 0.08	12.21 ± 0.33
K^+K^-	16.88 ± 0.22	16.90 ± 0.20	17.72 ± 0.52
Total (< 1.05 GeV)	567.00 ± 1.63	569.04 ± 1.08	570.68 ± 3.67

References

- [1] Davier M, Eidelman S, Hoecker A and Zhang Z 2003 *Eur.Phys.J. C* **27** 497
- [2] Davier M, Eidelman S, Hoecker A and Zhang Z 2003 *Eur.Phys.J. C* **31** 503
- [3] Davier M 2007 *Nucl. Phys. Proc. Suppl.* **169** 288
- [4] Davier M, Hoecker A, Malaescu B and Zhang Z 2011 *Eur.Phys.J. C* **71** 1515 (preprint arxiv:1010.4180)
- [5] Benayoun M, David P, DelBuono L, Leitner O and O'Connell H B 2008 *Eur.Phys.J. C* **55** 199-236 (preprint hep-ph/0711.4482)
- [6] Jegerlehner F and Szafron 2011 *Eur. Phys. J. C* **71** 1632 (preprint arXiv:1101.2872)
- [7] Davier M, Hoecker A, Lopez Castro G, Malaescu B, Mo, X H, Toledo Sanchez G, Wang P, Yuan C Z and Zhang Z 2010 *Eur. Phys. J. C* **66** 127-136 (preprint arxiv:0906.5443)
- [8] Harada M and Yamawaki K 2003 *Phys. Rept.* **381** 1-233 (preprint hep-ph/0302103)
- [9] Benayoun M, David P, DelBuono, L and Jegerlehner F 2012 *Eur.Phys.J. C* **72** 1848 (preprint arXiv:1106.1315)
- [10] Fujiwara T, Kugo T, Terao, H, Uehara S and Yamawaki K 1985 *Prog. Theor. Phys.* **73** 926-941
- [11] Bando M, Kugo T and Yamawaki, K 1985 *Nucl. Phys. B* **259** 493-502
- [12] Hashimoto M 1996 *Phys. Rev. D* **54** 5611-5619
- [13] Benayoun M and O'Connell H B 1998 *Phys. Rev. D* 074006
- [14] 't Hooft G 1986 *Phys. Rept.* **142** 357-387
- [15] Marciano W J and Sirlin A 1993 *Phys. Rev. Lett.* **71** 3629-3632
- [16] Cirigliano V, Ecker G and Neufeld H 2001 *Phys. Lett B* **513** 361-370 (preprint hep-ph/0104267)
 Cirigliano V, Ecker G and Neufeld H 2002 *JHEP* **08** 002 (preprint hep-ph/027310)
- [17] Benayoun M, David P, DelBuono, L and Jegerlehner F 2013 *Eur.Phys.J. C* **73** 2453 (preprint arXiv:1210.7184)
- [18] Beringer J *et al.* 2012 Review of Particle Physics (RPP) *Phys.Rev. D* **86** 010001
- [19] Aulchenko V M *et al.* 2002 *Phys. Lett. B* **527** 161-172 (preprint hep-ex/0112031)
 Akhmetshin R R *et al.* 2006 *Phys. Lett. B* **648** 28-38 (preprint hep-ex/0610021)
 Akhmetshin R R *et al.* 2006 *JETP Lett.* **84** 413-417 (preprint hep-ex/0610016)
- [20] Achasov M N *et al.* 2006 *JJ. Exp. Theor. Phys.* **103** 380-384 (preprint hep-ex/0605013)
- [21] Venanzoni G *et al.* 2009 *AIP Conf. Proc.* **1182** 665 (preprint arXiv:0906.4331)
- [22] Ambrosino F *et al.* 2011 *Phys. Lett. B* **700** 102-110 (preprint arXiv:1006.5313)
- [23] Babusci D *et al.* 2013 *Phys. Lett. B* **720** 336-343 (preprint arXiv:1212.4524)
- [24] Aubert B *et al.* 2009 *Phys. Rev. Lett.* **103** 231801 (preprint arXiv:0908.3589)
 Lees J P *et al.* 2012 *Phys. Rev. D* **86** 032013 (preprint arXiv:1205.2228)
- [25] Ablikim M *et al.* 2015 (preprint arXiv:1507.08188)
- [26] Benayoun M 2014 *Int.J.Mod.Phys.Conf.Ser.* **35** 1460416; Benayoun M 2013 *PoS Photon2013* 048
- [27] Benayoun M, David P, DelBuono, L and Jegerlehner F 2015 (preprint arXiv:1507.02943)
- [28] Schael S *et al.* 2005 *Phys. Rept.* **421** 191-284
- [29] Anderson S *et al.* 2000 *Phys. Rev. D* **61** 112002 (preprint hep-ex/9910046)
- [30] Fujikawa M *et al.* 2008 *Phys. Rev. D* **78** 072006 (preprint arXiv:0805.3773)
- [31] Barkov L M *et al.* 1985 *Nucl. Phys. B* **256** 365-384
- [32] Davier M, Hoecker A, Malaescu B, Yuan C-Z and Zhang Z 2014 *Eur.Phys.J. C* **74** 2803 (preprint arXiv:1312.1501)